Published in final edited form as:
Chromosoma. 2004 June ; 112(8): 398–409.

Targeting SMN to Cajal bodies and nuclear gems during neuritogenesis

Joaquin Navascues, **Maria T. Berciano**, and **Miguel Lafarga**
Department of Anatomy and Cell Biology, Biomedicine Unit, CSIC, University of Cantabria, Santander, Spain e-mail: lafargam@unican.es

Karen E. Tucker and **A. Gregory Matera**
Department of Genetics, Case Western Reserve University, 10900 Euclid Ave, Cleveland, OH 44106-4955, USA e-mail: a.matera@case.edu

Abstract

Neurite outgrowth is a central feature of neuronal differentiation. PC12 cells are a good model system for studying the peripheral nervous system and the outgrowth of neurites. In addition to the dramatic changes observed in the cytoplasm, neuronal differentiation is also accompanied by striking changes in nuclear morphology. The large and sustained increase in nuclear transcription during neuronal differentiation requires synthesis of a large number of factors involved in pre-mRNA processing. We show that the number and composition of the nuclear subdomains called Cajal bodies and gems changes during the course of N-*ras*-induced neuritogenesis in the PC12-derived cell line UR61. The Cajal bodies found in undifferentiated cells are largely devoid of the survival of motor neurons (SMN) protein product. As cells shift to a differentiated state, SMN is not only globally upregulated, but is progressively recruited to Cajal bodies. Additional SMN foci (also known as Gemini bodies, gems) can also be detected. Using dual-immunogold labeling electron microscopy and mouse embryonic fibroblasts lacking the coilin protein, we show that gems clearly represent a distinct category of nuclear body.

Introduction

An important aspect of neuronal differentiation is the generation of axons and dendrites. Their outgrowth is, therefore, a critical process in the formation of neuronal networks (Kandel et al. 2000). Concomitant with production of these long cytoplasmic processes is a large and sustained increase in nuclear transcription and cell body size (Santama et al. 1996). In order to meet this new demand, factors involved in pre-mRNA processing must also be synthesized. Cajal bodies (CBs) are nuclear structures involved in the biogenesis of RNA-processing factors (Verheggen et al. 2002; Jady et al. 2003) and are prominent features of mammalian neurons (Cajal 1910; Lafarga et al. 1983; Peters et al. 1991; Pena et al. 2001). While little is known about nuclear remodeling events during neuronal differentiation, late-stage neurons are characterized by larger cell bodies with smaller and diffusely organized splicing factor compartments (Pena et al. 2001). The early stage, smaller neurons have fewer but larger splicing factor compartments (speckles), consistent with their relative transcriptional quiescence as compared with the larger neurons (Pena et al. 2001). Moreover, the number of CBs per cell is upregulated as neuronal cell body size increases (Lafarga et al. 1991, 1998; Pena et al. 2001). The composition of CBs can also change during development. Morris and colleagues showed that the survival of motor neurons (SMN) protein complex colocalizes with coilin, the CB signature protein, in adult cells and tissues (Young et al. 2000), whereas the two

Correspondence to: Miguel Lafarga.Correspondence to: A. Gregory Matera.

factors appear as independent nuclear bodies during embryonic development (Young et al. 2001). The colocalization of SMN and coilin progressively increases with fetal age, suggesting that recruitment of SMN to CBs is developmentally regulated (Young et al. 2001). Thus, stage-specific changes in nuclear organization, similar to the well-documented rearrangements of cytoplasmic components, are important, pre-programmed aspects of neuronal differentiation.

The rat pheochromocytoma cell line, PC12, is a useful model system for studying many cell-signaling pathways, especially those leading to neuritogenesis, a cellular hallmark of neuronal differentiation (Vaudry et al. 2002). The current view is that differentiation is produced not by induction of entirely novel signaling pathways for a given cell fate, but rather from unique combinations of canonical signaling cassettes. Accordingly, differentiation of PC12 cells by nerve growth factor (NGF) proceeds through the Raf → mitogen activated kinase kinase → extracellular signal-regulated kinase pathway (reviewed in Vaudry et al. 2002). Somewhat paradoxically, the products of the *src* and *ras* oncogenes do not promote proliferation of PC12 cells (Bar-Sagi and Feramisco 1985; Noda et al. 1985; D'Arcangelo and Halegoua 1993). Rather, they enhance NGF-mediated differentiation through a receptor tyrosine kinase called TrkA (reviewed in Chao and Hempstead 1995). Guerrero et al. (1988) capitalized on these findings to create a stable PC12 subline, called UR61, that contains a mouse N-*ras* gene driven by a dexamethasone-inducible promoter. Treatment of UR61 cells with 0.2 μM dexamethasone for 24 h causes outgrowth of neurites and halts proliferation. UR61 cells display a great deal of cellular homogeneity in terms of cell size and general morphology, making them an ideal model system to study the organization and composition of nuclear bodies during neuronal differentiation.

In this study, we describe how changes in gene expression associated with neuron-like differentiation of UR61 cells correlate with alterations in the number and composition of CBs and their twin SMN-positive, coilinnegative structures, called Gemini bodies (gems). The results show that most undifferentiated cells contain coilinpositive CBs that lack SMN. Furthermore, gems are very rare in proliferating UR61 cells. As the cells shift from a proliferative to a differentiated state in response to dexamethasone treatment, SMN is progressively recruited to CBs. Unlike the situation in adult tissues or explanted adult neurons (Pena et al. 2001; Young et al. 2001), differentiated UR61 cells also display an increased number of gems. This abundance of gems allowed us to characterize the ultrastructure of this nuclear inclusion, revealing the existence of a morphologically distinct nuclear body. Immunoblotting analysis of treated and untreated cells showed that SMN is globally upregulated by N-*ras* induction and that the increase in nuclear accumulation of SMN in the CBs of differentiated cells occurs without depletion of the cytoplasmic pool. Transient expression of green fluorescent protein (GFP)-SMN in undifferentiated UR61 cells promoted the cytoplasmic accumulation of SMN and the recruitment of GFP-SMN to nuclear CBs, but did not induce formation of gems. Gem formation was induced, however, upon treatment of differentiated UR61 cells with methyltransferase inhibitors. Collectively, these results reveal the dynamic nature of the interplay between nuclear sub-compartments during neuronal development.

Materials and methods

Cell culture, transfection assays and treatments

The UR61 cells were cultured in RPMI 1640 medium supplemented with 10% normal calf serum, 100 units/ml gentamycin, as described previously (Greene and Tischer 1976), and grown on coverslips. To induce neuron-like differentiation, cultures were exposed to 0.2 μM dexamethasone for 12, 24, 36 and 48 h (Guerrero et al. 1988). Transfection was performed with the plasmid construct pGFP-SMN, as previously described (Shpargel et al. 2003; Sleeman et al. 2003). Untreated and dexamethasone-treated UR61 cells were transfected for 18 h using

FuGene 6 transfection reagent (Roche) according to the manufacturer's instructions. For drug treatments, undifferentiated and differentiated UR61 cells were incubated for 24 h with the vehicle (DMSO) or with the methyltransferase inhibitors 5′-deoxy-5′-methylthioadenosine (MTA, Sigma), at a final concentration of 750 μM (Boisvert et al. 2002), or with 100 μM adenosine dialdehyde (AdOx, Sigma), as previously reported (Young et al. 2001).

Fluorescence microscopy and immunostaining

The UR61 cells grown on coverslips were fixed for 10 min in 3.7% paraformaldehyde in phosphate-buffered saline (PBS). Then cells were permeabilized with 0.5% Triton X-100 for 10 min, blocked with 1% normal goat serum for 10 min, incubated with primary antibodies for 1 h, washed in PBS and incubated with the secondary antibodies (Jackson Laboratories). Some cell samples were stained with fluorescein isothiocyanate (FITC)-conjugated phalloidin (Sigma). After several washes, cells were mounted in Vectashield medium (Vector Laboratories). Primary antibodies used were anti-coilin 204.10 rabbit serum (Bohmann et al. 1995), anti-SMN monoclonal antibody (mAb) (Transduction Laboratories), anti-SMN 2B1 mAb (Liu and Dreyfuss 1996), anti-Gemin2/SIP1 E17 mAb (Liu et al. 1997), anti-Sm C45 human serum, anti-U2B" 4G3 mAb, and anti-Nopp 140 rabbit serum RF12 (Meier and Blobel 1992). Cell samples were examined using a Zeiss 63× NA 1.4 PlanApo objective. Images were recorded using a BioRad MRC 1024 confocal laser scanning microscope equipped with argon (488 nm) and HeNe (543 nm) lasers.

Immunoelectron microscopy

For immunoelectron microscopy, UR61 and coilin knockout mouse embryonic fibroblasts (MEFs; Tucker et al. 2001) were fixed with 4% paraformaldehyde in 0.1 M cacodylate buffer for 1 h at room temperature. The cells were scraped from the dishes, transferred to an Eppendorf tube, and centrifuged for 1 min in a microfuge to pellet the cell cultures. The pellets were washed with 0.1 M cacodylate buffer, dehydrated in increasing concentrations of methanol at -20°C, embedded in Lowicryl K4M at -20°C and polymerized with ultraviolet irradiation. Ultrathin sections were mounted on nickel grids and sequentially incubated with 0.1 M glycine in PBS for 15 min, 5% BSA in PBS for 30 min and the primary antibody (diluted in 50 mM TRIS-HCl, pH 7.6, containing 1% BSA and 0.1 M glycine) for 1 h at 37°C. After washing, the sections were incubated with goat anti-rabbit IgG coupled to 10 nm or 15 nm gold particles (BioCell, UK; diluted 1:50 in PBS containing 1% BSA). For double immunoelectron microscopy, ultrathin sections were sequentially incubated with anti-SMN and anti-coilin antibodies and then with the specific secondary antibodies coupled to 10 nm and 15 nm gold particles. Following immunogold labeling, the grids were stained with lead citrate and uranyl acetate and examined with a Phillips EM208 electron microscope operated at 60 kV. As controls, ultrathin sections were treated as described above but omitting primary antibodies. Primary antibodies used were anti-coilin 204.10 rabbit serum, anti-SMN 2B1 mAb (courtesy G. Dreyfuss) and anti-SMN mAb (Transduction Laboratories).

Subcellular fractionation and immunoblotting

For subcellular fractionation, UR61 cells were washed in PBS, counted with a Neubauer chamber and lysed in cold Buffer A (10 mM HEPES, pH 7.9, 10 mM KCl, 1.5 mM $MgCl_2$) supplemented with 1 μg/ml leupeptin, 1 μg/ml aprotinin and 0.5 mM phenylmethylsulfonyl fluoride (PMSF) and containing 2.5% Nonidet P-40 for 30 min on ice. The lysate was centrifugated at 3500 rpm for 4 min at 4°C. Supernatants were taken as cytosolic fraction. Pellets (nuclei) were incubated on ice in Buffer C (20 mM HEPES, pH 7.9, 0.45 M NaCl, 1 mM EDTA) supplemented with 1 μg/ml leupeptin, 1 μg/ml aprotinin and 0.5 mM PMSF for 20 min. Cellular debris was removed by centrifugation at 14,000 rpm for 10 min at 4°C, and the supernatant was taken as nuclear fraction. Subcellular extracts from 300,000 cells per lane

were used. Proteins were separated on SDS-polyacrylamide gels and transferred to nitrocellulose membranes by standard procedures. The following primary antibodies were used: mouse monoclonal anti-tyrosine hydroxylase 22941 (Incstar Corporation), mouse monoclonal anti-SMN (clone 8, Transduction Laboratories) and rabbit polyclonal serum raised against a peptide corresponding to the carboxy-terminal end of human fibrillarin (Jansen et al. 1991). Immunoblots were visualized by chemiluminescence (ECL, Amersham).

Results

Guerrero et al. (1988) have shown by phase contrast microscopy that dexamethasone treatment induces differentiation of UR61 cells into a sympathetic neuron-like appearance. In order to extend these observations and toshow that UR61 cells represent a good model system for mimicking NGF-mediated differentiation, we used three different methods to illustrate distinct hallmarks of neuronal differentiation in dexamethasone-treated cells. First, we used FITC-conjugated phalloidin to demonstrate the presence of actin in the growing neurites of cells treated with dexamethasone for 36-48 h (Fig. 1). Undifferentiated UR61 cells have a globular morphology, with numerous blebs at the surface of the plasma membrane (Fig. 1a). Dexamethasone treatment induces enlargement of the cell bodies, disappearance of membrane blebs and development of multiple cytoplasmic processes that progressively branch and grow (Fig. 1b,c). A second criterion for differentiation of sympathetic-type neurons is the upregulation of tyrosine hydroxylase (TH), a key enzyme in catecholamine biosynthesis. The TH gene promoter contains a glucocorticoid response element (Hagerty et al. 2001), and the accumulation of TH in the cytoplasmic region of the cell body is clearly induced upon treatment of UR61 cells with dexamethasone (Fig. 1d-f). Third, synthesis of catecholamines such as dopamine results in the cytoplasmic accumulation of secretory granules, as observed in the electron microscope (Tischler and Greene 1978). Accordingly, we observed numerous dense secretory granules in the cytoplasm of dexamethasone-treated cells that were largely absent in untreated cells (Fig. 1g,h). Thus, dexamethasone treatment induces a high degree of differentiation, making UR61 cells a good model system to study the subcellular organization of coilin and SMN during neuritogenesis.

Differentiation induces accumulation of SMN in Cajal bodies and nuclear gems

We analyzed coilin and SMN staining in UR61 cells by immunofluorescence during a course of dexamethasoneinduced differentiation. Cells were fixed at 0, 12, 24, 36 and 48 h following exposure to dexamethasone and the number of nuclear bodies containing coilin, SMN or both proteins was counted. As shown in Fig. 2, untreated cells primarily contain CBs that are coilin positive and SMN negative. Expression of SMN is relatively low and largely restricted to the cytoplasm. Furthermore, gems (SMN-positive, coilin-negative foci) are very rare in untreated cells. As differentiation proceeds, the number of CBs containing both coilin and SMN progressively increases, with a concomitant decrease in the number of coilin-only foci (Fig. 2c). In fact, after 48 h of dexamethasone treatment, nearly all of the differentiated cells contained CBs that were positive for both SMN and coilin (Fig. 2b and data not shown). Furthermore, over half of the total number of nuclear bodies were doubly positive for coilin and SMN (Fig. 2c). Thus, neuronal differentiation of UR61 cells results not only in a general upregulation of SMN expression (as measured by immunoblotting, see below), but in recruitment of SMN protein to CBs.

In order to demonstrate that the coilin foci observed in dexamethasone-treated cells are bona fide CBs, we performed immunofluorescence with antibodies targeted against various CB constituents, including coilin, SMN, Gemin2, SmB, U2B” and Nopp140. As shown in Fig. 3, cells treated with dexamethasone for 36 h displayed coilin foci that colocalized to varying degrees with those of other CB constituents. Consistent with the observations in Fig. 1, members of the SMN complex often colocalized completely with coilin (Fig. 3a,c,d,g). In a

subset of cells, independent nuclear bodies (gems) were observed (Fig. 3b,e). As originally shown in a HeLa (PV) subline (Liu and Dreyfuss 1996), the gems in UR61 cells were completely devoid of detectable Sm proteins or other spliceosomal components (Fig. 3i and data not shown).

Ultrastructural characterization of gems

Since their discovery in 1996, gems have been identified only at the level of the light microscope (Liu and Dreyfuss 1996) and thus their ultrastructural identification has remained elusive. We took advantage of the abundance of gems in differentiated UR61 cells to characterize their structure by immunogold electron microscopy. We used rabbit polyclonal anti-coilin and mouse monoclonal anti-SMN antibodies in a dual-labeling approach. Secondary antibodies were conjugated with 10 nm and 15 nm gold particles for detection of SMN and coilin, respectively. In dexamethasone-treated cells, most of the labeled nuclear bodies displayed the typical pattern of colocalization of SMN and coilin on the dense threads that distinguish CBs from other bodies (Fig. 4a). As previously observed in the CBs of Huh7 cells (Carvalho et al. 1999), the coilin and SMN signals were intermingled throughout the CB. However, a subset of the labeled nuclear bodies contained only 10 nm (SMN) gold particles. These appeared as round bodies with a granular texture and intermediate electron density, ranging from 0.2 to 0.4 μm in diameter (Fig. 4b). In order to confirm that these structures were indeed gems, we performed immunogold labeling on MEF cells that do not contain coilin. The SMN in this cell line, called MEF42, accumulates in gems in a subset of cells (10-20%) and CBs are completely absent (Tucker et al. 2001). As shown in Fig. 4c, the fine structure of the gems in MEF42 cells is indistinguishable from that observed in UR61 cells (compare Fig. 4b,c). Occasionally we observed structures that appeared to be CB-gem pairs, with coilin signals on the dark threads and SMN labeling the dark, granular material (Fig. 4d). As previously described (Lafarga et al. 1998; Pena et al. 2001), we also identified CBs juxtaposed with an amorphous material that failed to label with either coilin or SMN (Fig. 4e). These unlabeled structures are likely to be CstF bodies (Schul et al. 1996; Gall 2000). In summary, the specific morphological characteristics revealed by these ultrastructural studies clearly demonstrate that gems represent a distinct category of nuclear body.

Dexamethasone-induced differentiation upregulates nuclear and cytoplasmic SMN levels

Having established the fine structure of gems, we next investigated whether the observed increase in their number in differentiating UR61 cells was due to a general upregulation of SMN protein or if it simply reflected a nuclear translocation event. We therefore performed immunoblot analysis to quantify the relative amounts of nuclear and cytoplasmic SMN. Tyrosine hydroxylase, a cytoplasmic protein that is known to be induced by dexamethasone, was used a control. As shown in Fig. 5, the levels of both nuclear and cytoplasmic SMN increased by ~50% upon treatment with dexamethasone. In contrast, tyrosine hydroxylase showed a much more dramatic change in the cytoplasm, boasting a ~70-fold increase. Moreover, the control blot also shows that cytoplasmic contamination of the nuclear fractions was minimal, as very little tyrosine hydroxylase was detected in this compartment. Similarly, little nuclear leakage was detected, as shown by the cytoplasmic fractions of the fibrillarin immunoblot (Fig. 5). In conclusion, the immunoblot analyses clearly show that the increase in SMN nuclear import occurs without significant depletion of the cytoplasmic pool.

Overexpression of GFP-SMN in undifferentiated UR61 cells does not stimulate gem formation

The general upregulation of SMN levels during dexamethasone treatment and concomitant increase in the number of gems suggested that these two features might be linked. Thus overexpression of SMN in undifferentiated UR61 cells might plausibly saturate the number of

CB-binding sites and lead to formation of gems. In fact, previous investigations using HeLa cells had shown that overexpression of wild-type SMN can lead to production of additional nuclear and cytoplasmic SMN foci (Shpargel et al. 2003; Sleeman et al. 2003). We therefore transiently expressed GFP-SMN in uninduced UR61 cells and monitored the number of CBs using anti-coilin antibodies. Surprisingly, we found that essentially all of the nuclear GFP-SMN foci in transfected cells contained coilin (Fig. 6a-c), and that coilin-positive bodies lacking GFP-SMN were not observed. A statistical analysis of the mean number of CBs in transfected (1.79±0.14) versus untransfected (1.65±0.25) cells showed no significant differences (*n*=200 cells). Thus transient expression of GFP-SMN in undifferentiated UR61 cells resulted in complete colocalization of nuclear SMN and coilin foci.

We also assayed the effects of GFP-SMN expression on differentiating cells. When UR61 cells were treated with dexamethasone for 20 h prior to transfection and then analyzed 20 h post-transfection, we found no significant difference in the number of CBs per cell (*n*=200 cells) in transfected versus untransfected cells (2.07±0.14 vs 2.00 ±0.23). As shown in Fig. 6, cells expressing either moderate (Fig. 6d-f) or high levels (Fig. 6g-i) of GFP-SMN showed no additional SMN-positive nuclear bodies, although cytoplasmic accumulations were readily detectable (Shpargel et al. 2003;Sleeman et al. 2003). Moreover,GFP-SMN expression did not affect the timecourse of differentiation toward a neuron-like phenotype. When undifferentiated UR61 cells were treated with dexamethasone and simultaneously transfected with GFP-SMN, we found that the progression of differentiation occurred normally and that transfected cells displayed typical neurites (Fig. 6j,k). Therefore, our results suggest that GFP-SMN overexpression in dexamethasone-treated cells does not interfere with the progression of neuritogenesis.

Methyltransferase inhibitors induce formation of nuclear bodies in differentiated UR61 cells

Since localization of SMN to CBs depends upon the methylation status of the coilin protein (Hebert et al. 2002; Boisvert et al. 2002), we wanted to assay the composition of CBs under conditions of reduced methyltransferase activity. We therefore investigated the effects of methylation inhibitors MTA and AdOx on the organization of CBs and gems in differentiated UR61 cells. The cells were exposed to dexamethasone for 40 h, then incubated for 4 h or 24 h in the presence of 750 μM MTA. Control cells were not treated with dexamethasone. Upon treatment for 24 h with MTA, differentiated UR61 cells showed a slight increase in SMN staining in the cytoplasm, along with a dramatic increase in the number of gems (Fig. 7a-c and Table 1). A small, but significant decrease in the number of CBs (coilin foci) was also observed, which in many cells was coupled with the relocalization of coilin into perinucleolar caps (Fig. 7d-f). Similar effects were observed in undifferentiated UR61 cells upon treatment with MTA, although, curiously, the increase in the number of gems was less dramatic. Shorter treatments with MTA (4 h) had little effect on the number of nuclear bodies in differentiated or undifferentiated cells (Table 1).

In contrast to the results obtained with MTA, differentiated UR61 cells incubated in the presence of 100 μM AdOx, showed little propensity for gem formation (Fig. 7g-l). Instead, the number of CBs increased from ~2 to ~3 per cell (Table 1), whereas the number of gems remained constant. This lack of gem formation in the presence of AdOx is consistent with previous observations in HeLa cells (Hebert et al. 2002; Boisvert et al. 2002). We do not currently understand the reasons why MTA is more efficient than AdOx at inducing gem formation. However, it is noteworthy that the two inhibitors likely act at different points along the methylation pathway.

Discussion

We have shown that SMN is upregulated during neuritogenesis in the PC12-derived, dexamethasone-inducible UR61 cell line. In undifferentiated UR61 cells, SMN is primarily cytoplasmic and does not localize to CBs, which are readily detectable by coilin staining. As differentiation proceeds, SMN is progressively recruited to CBs. Whereas gems (SMN-positive, coilin-negative foci) are extremely rare in undifferentiated cells, they are more readily detected upon differentiation (Fig. 2). Quantitative immunoblotting analysis reveals that SMN levels are upregulated to similar extents in both the nucleus and cytoplasm (Fig. 5). Thus the increase in nuclear SMN is not due to a decrease in the cytoplasmic pool of the protein and is therefore likely a general effect.

This global upregulation of SMN and concomitant formation of nuclear gems in differentiated UR61 cells was plausibly the result of a titration of the available CB binding sites in the nucleus, leading to the aggregation of SMN in a separate nuclear body. We envision that gems are much less complex than CBs, consisting entirely of SMN and it's "core" binding factors (Gemins 2-7), as Sm proteins and other snRNP epitopes are completely undetectable in these structures. We were, therefore, surprised when we overexpressed GFP-SMN in undifferentiated UR61 cells and found that gem formation was not induced. Instead, we found that essentially all of the nuclear GFP-SMN was colocalized in CBs with coilin in undifferentiated cells. It is possible, given the relative dearth of SMN-positive CBs, that there is a surplus of symmetrically dimethylated coilin molecules (either with-in CBs or in the nucleoplasm) in these cells. The relative lack of gems in undifferentiated cells and their presence following dexamethasone treatment might reflect an inherent difference in the regulation of nuclear SMN levels. Perhaps the nuclear SMN is more rapidly degraded or shuttled back out to the cytoplasm in undifferentiated versus differentiated cells.

Surprisingly, the total number of nuclear bodies was similarly refractive to GFP-SMN overexpression in dexamethasone-treated UR61 cells. These findings are curious because high levels of overexpression of myc-tagged and GFP-tagged SMN in HeLa cells resulted in a large increase in the numbers of both nuclear and cytoplasmic SMN foci (Hebert et al. 2002; Shpargel et al. 2003; Sleeman et al. 2003). While it is possible that similar high levels of SMN overexpression cannot be achieved in UR61 cells, it appears that differentiation-induced formation of gems in UR61 is not simply the result of increased SMN expression levels.

The fine structure of gems

To date, gems have only been characterized at the light microscope level. From a purely morphological standpoint, one important question that has occupied the nuclear body field for some time is whether or not gems actually have an electron-dense substructure. Through the use of dual-immunogold labeling, Carvalho et al. (1999) showed that coilin and SMN signals are intermingled throughout the dark threads that characterize the CB. However, no SMN-positive, coilin-negative bodies were observed in that study (Carvalho et al. 1999). We clearly showed that a fraction of the SMN foci in differentiated UR61 cells are coilin negative at both the light and electron microscope level (Figs. 2,4, respectively). Dual labeling revealed the existence of SMN-positive, coilin-negative nuclear bodies of intermediate electron density, bearing a granular texture and ranging in size from around 0.2-0.4 μm in diameter (Fig. 4). We confirmed that these structures indeed correspond to gems through the use of MEF cells derived from coilin knockout mice. Nuclear SMN is entirely restricted to gems in coilin knockout MEFs, as these cells do not contain CBs (Tucker et al. 2001). The SMN-positive, coilin-negative structures in UR61 cells were ultrastructurally indistinguishable from those in the MEFs. In agreement with these findings, Malatesta et al. (2004) recently showed that SMN accumulates in granular structures that are almost certainly gems. While these investigators did not perform double labeling to exclude the possibility of coilin colocalization, the similar

morphology and frequent juxtaposition with bona fide CBs make the strong case that the structures observed by Malatesta et al. (2004) are indeed gems. In summary, multiple cellular model systems demonstrate that nuclear accumulation of the SMN complex results in formation of a detectable nuclear body.

Acknowledgements

Acknowledgements This work was supported by grants from the following institutions: Centro de Investigación de Enfermedades Neurológicas (CIEN), Instituto de Salud Carlos III (Madrid, Spain); Dirección General de Investigacion of Spain (BFI2002-0454); the National Institutes of Health, USA (R01-NS41617 and R01-GM53034) and the Muscular Dystrophy Association, USA (RG 3290).

References

Bar-Sagi D, Feramisco JR. Microinjection of the ras oncogene protein into PC12 cells induces morphological differentiation. Cell 1985;42:841–848. [PubMed: 2996779]

Bohmann K, Ferreira JA, Lamond AI. Mutational analysis of p80 coilin indicates a functional interaction between coiled bodies and the nucleolus. J Cell Biol 1995;131:817–831. [PubMed: 7490287]

Boisvert FM, Cote J, Boulanger MC, Cleroux P, Bachand F, Autexier C, Richard S. Symmetrical dimethylarginine methylation is required for the localization of SMN in Cajal bodies and pre-mRNA splicing. J Cell Biol 2002;159:957–969. [PubMed: 12486110]

Cajal SR. El núcleo de las células piramidales del cerebro humano y de algunos mamíferos. Trab Lab Invest Biol 1910;8:27–62.

Carvalho T, Almeida F, Calapez A, Lafarga M, Berciano MT, Carmo-Fonseca M. The spinal muscular atrophy disease gene product, SMN: a link between snRNP biogenesis and the Cajal (coiled) body. J Cell Biol 1999;147:715–727. [PubMed: 10562276]

Chao MV, Hempstead BL. p75 and Trk: a two-receptor system. Trends Neurosci 1995;18:321–326. [PubMed: 7571013]

D'Arcangelo G, Halegoua S. A branched signaling pathway for nerve growth factor is revealed by Src-, Ras-, and Raf-mediated gene inductions. Mol Cell Biol 1993;13:3146–3155. [PubMed: 8497245]

Gall JG. Cajal bodies: the first 100 years. Annu Rev Cell Dev Biol 2000;16:273–300. [PubMed: 11031238]

Greene LA, Tischler AS. Establishment of a noradrenergic clonal line of rat adrenal pheochromocytoma cells which respond to nerve growth factor. Proc Natl Acad Sci USA 1976;73:2424–2428. [PubMed: 1065897]

Guerrero I, Pellicer A, Burstein DE. Dissociation of c-Fos from ODC expression and neuronal differentiation in a PC12 subline stably transfected with an inducible N-*ras* oncogene. Biochem Biophys Res 1988;150:1185–1192.

Hagerty T, Morgan WW, Elango N, Strong R. Identification of a glucocorticoid-responsive element in the promoter region of the mouse tyrosine hydroxylase gene. J Neurochem 2001;76:825–834. [PubMed: 11158254]

Hebert MD, Shpargel KB, Ospina JK, Tucker KE, Matera AG. Coilin methylation regulates nuclear body formation. Dev Cell 2002;3:329–337. [PubMed: 12361597]

Jady BE, Darzacq X, Tucker KE, Matera AG, Bertrand E, Kiss T. Modification of Sm small nuclear RNAs occurs in the nucleoplasmic Cajal body following import from the cyto-plasm. EMBO J 2003;22:4283–4293. [PubMed: 12912925]

Jansen RP, Hurt EC, Kern H, Lehtonen H, Carmo-Fonseca M. Evolutionary conservation of the human nucleolar protein fibrillarin and its functional expression in yeast. J Cell Biol 1991;113:715–729. [PubMed: 2026646]

Kandel, ER.; Schwartz, JH.; Jessell, TM. Principles of neural science. McGraw-Hill Company; New York: 2000.

Lafarga M, Hervas JP, Santa-Cruz MC, Villegas J, Crespo D. The "accessory body" of Cajal in the neuronal nucleus. A light and electron microscopic approach. Anat Embryol 1983;166:19–30. [PubMed: 6301310]

Lafarga M, Andres MA, Berciano MT, Maquiera E. Organization of nucleoli and nuclear bodies in osmotically stimulated supraoptic neurons of the rat. J Comp Neurol 1991;308:329–339. [PubMed: 1865004]

Lafarga M, Berciano MT, Garcia-Segura LM, Andres MA, Carmo-Fonseca M. Acute osmotic/stress stimuli induce a transient decrease of transcriptional activity in the neurosecretory neurons of supraoptic nuclei. J Neurocytol 1998;27:205–217. [PubMed: 10640180]

Liu Q, Dreyfuss G. A novel nuclear structure containing the survival of motor neurons protein. EMBO J 1996;15:3555–3565. [PubMed: 8670859]

Liu Q, Fischer U, Wang F, Dreyfuss G. The spinal muscular atrophy disease gene product, SMN, and its associated protin SIP1 are in a complex with spliceosomal snRNP proteins. Cell 1997;90:1013–1021. [PubMed: 9323129]

Meier UT, Blobel G. Nopp 140 shuttles on tracks between nucleolus and cytoplasm. Cell 1992;70:127–138. [PubMed: 1623516]

Malatesta M, Scassellati C, Meister G, Plottner O, Buhler D, Sowa G, Martin TE, Keidel E, Fischer U, Fakan S. Ultrastructural characterisation of a nuclear domain highly enriched in survival of motor neuron (SMN) protein. Exp Cell Res 2004;292:312–321. [PubMed: 14697339]

Noda M, Ko M, Ogura A, Liu DG, Amano T, Tacano T, Ikawa Y. Sarcoma viruses carrying ras oncogenes induce differentiation-associated properties in a neuronal cell line. Nature 1985;318:73–75. [PubMed: 4058592]

Pena E, Berciano MT, Fernandez R, Ojeda JL, Lafarga M. Neuronal body size correlates with the number of nucleoli and Cajal bodies, and with the organization of the splicing machinery in rat trigeminal ganglion neurons. J Comp Neurol 2001;430:250–263. [PubMed: 11135260]

Peters, A.; Palay, SL.; Webster, H.; de, F. The fine structure of the nervous system. Neurons and their supporting cells. Oxford University Press; New York: 1991.

Santama N, Dotti CG, Lamond AI. Neuronal differentiation in the rat hippocampus involves a stage-specific reorganization of subnuclear structure both in vivo and in vitro. Eur J Neurosci 1996;8:892–905. [PubMed: 8743737]

Schul W, Groenhaut B, Koberna K, Takagaki Y, Jenny A, Manders EM, Raska I, van Driel R, de Jong L. The RNA 3' cleavage factors CstF 64 kDa and CPSF 100 kDa are concentrated in nuclear domains closely associated with coiled bodies and newly synthesized RNA. EMBO J 1996;15:2883–2892. [PubMed: 8654386]

Shpargel KB, Ospina JK, Tucker KE, Matera AG, Hebert MD. Control of Cajal body number is mediated by the coilin C-terminus. J Cell Sci 2003;14:9–16.

Sleeman JE, Trinkle-Mulcahy L, Prescott AR, Ogg SC, Lamond AI. Cajal body proteins SMN and coilin show differential dynamic behaviour in vivo. J Cell Sci 2003;116:2039–2050. [PubMed: 12679382]

Tischer AS, Greene LA. Morphologic and cytochemical properties of a clonal line of rat adrenal pheochromocytoma cells which respond to nerve growth factor. Lab Invest 1978;39:77–89. [PubMed: 682602]

Tucker KE, Berciano MT, Jacobs EY, LePage DF, Shpargel KB, Rossire J, Chan EKL, Lafarga M, Colon RA, Matera AG. Residual Cajal bodies in coilin knockout mice fail to recruit Sm snRNPs and SMN, the spinal muscular atrophy gene product. J Cell Biol 2001;154:293–307. [PubMed: 11470819]

Vaudry D, Stork JS, Lazarovici P, Eiden LE. Signaling pathways for PC12 cell differentiation: Making the right connections. Science 2002;296:1648–1649. [PubMed: 12040181]

Verheggen C, Lafontaine DL, Samarsky D, Mouaikel J, Blanchard JM, Bordonne R, Bertrand E. Mammalian and yeast U3 snoRNPs are matured in specific and related nuclear compartments. EMBO J 2002;21:2736–2756. [PubMed: 12032086]

Young PJ, Le TT, thi Man N, Burghes AH, Morris GE. The relationship between SMN, the spinal muscular atrophy protein, and nuclear coiled bodies in differentiated tissues and cultured cells. Exp Cell Res 2000;256:365–374. [PubMed: 10772809]

Young PJ, Le TT, Dunckley M, thi Man N, Burghes AH, Morris GE. Nuclear gems and Cajal (Coiled) bodies in fetal tissues: Nucleolar distribution of the spinal muscular atrophy protein, SMN. Exp Cell Res 2001;265:252–261. [PubMed: 11302690]

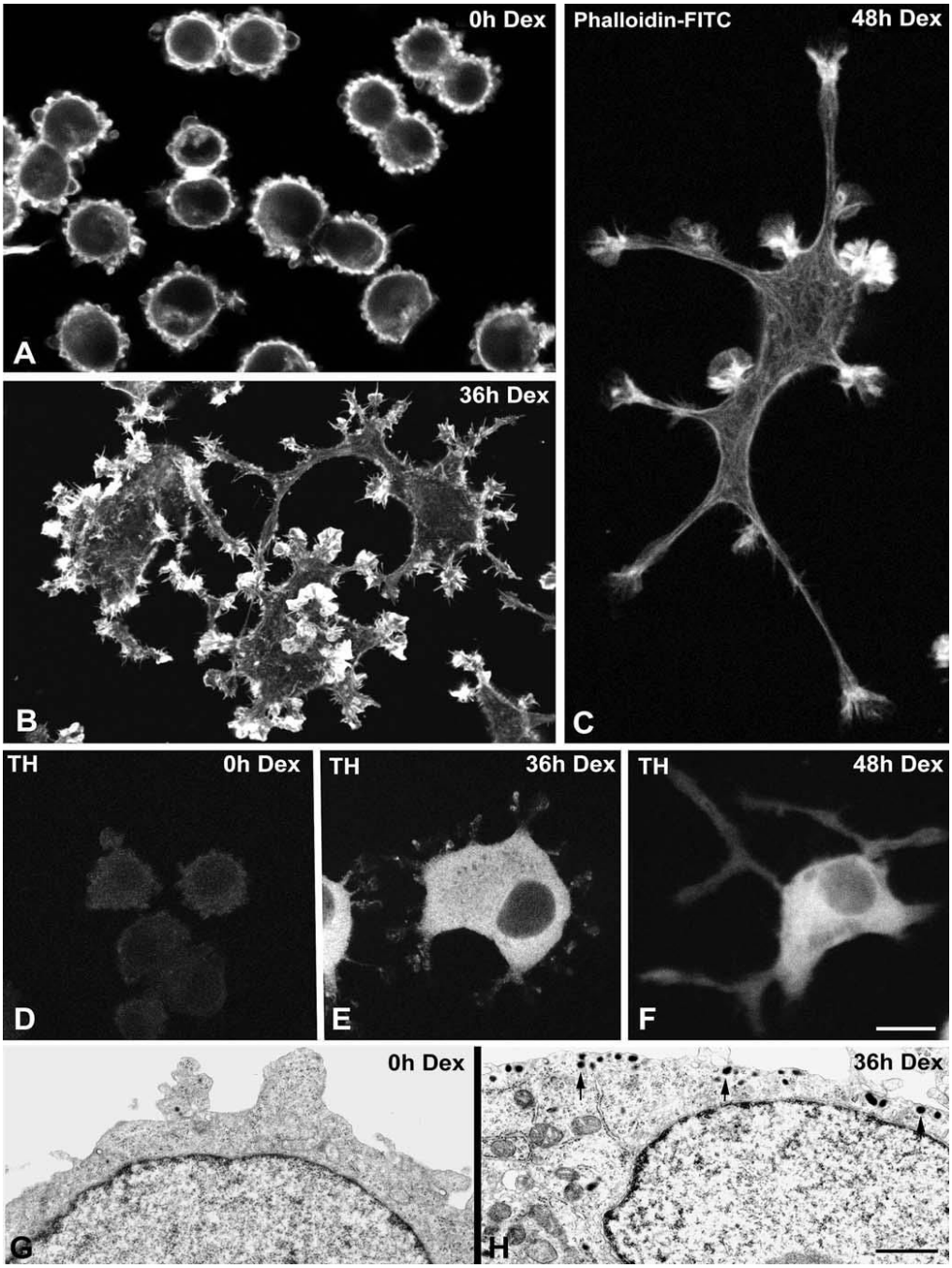

Fig. 1a-h.

Dexamethasone (Dex) treatment induces differentiation of UR61 cells into a sympathetic neuron-like phenotype. **a-c** Phalloidin-FITC (fluorescein isothiocyanate) was used as marker of cortical actin to demonstrate two progressive stages of neuritogenesis upon dexamethasone treatment for 36 h **b** and 48 h **c**. Untreated cells (**a**) exhibit a round shape with numerous blebs of the plasma membrane. **d-f** UR61 cells were stained for tyrosine hydroxylase (TH). Weak labeling is detected in the cytoplasm of untreated cells (**d**), but the cytoplasmic expression of this enzyme dramatically increases upon dexamethasone treatment (**e,f**). **g**, **h** Representative electron micrographs of untreated (**g**) and dexamethasone-treated (**h**) UR61 cells. Note in **g** the narrow band of perinuclear cytoplasm, the absence of secretory granules and the formation

of blebs at the cell cortex. Upon dexamethasone-induced differentiation (**h**) numerous secretory granules (arrows) appear, predominantly distributed in the marginal cytoplasm. Bar represents 5 μm(**a-f**); 1 μm(**g, h**)

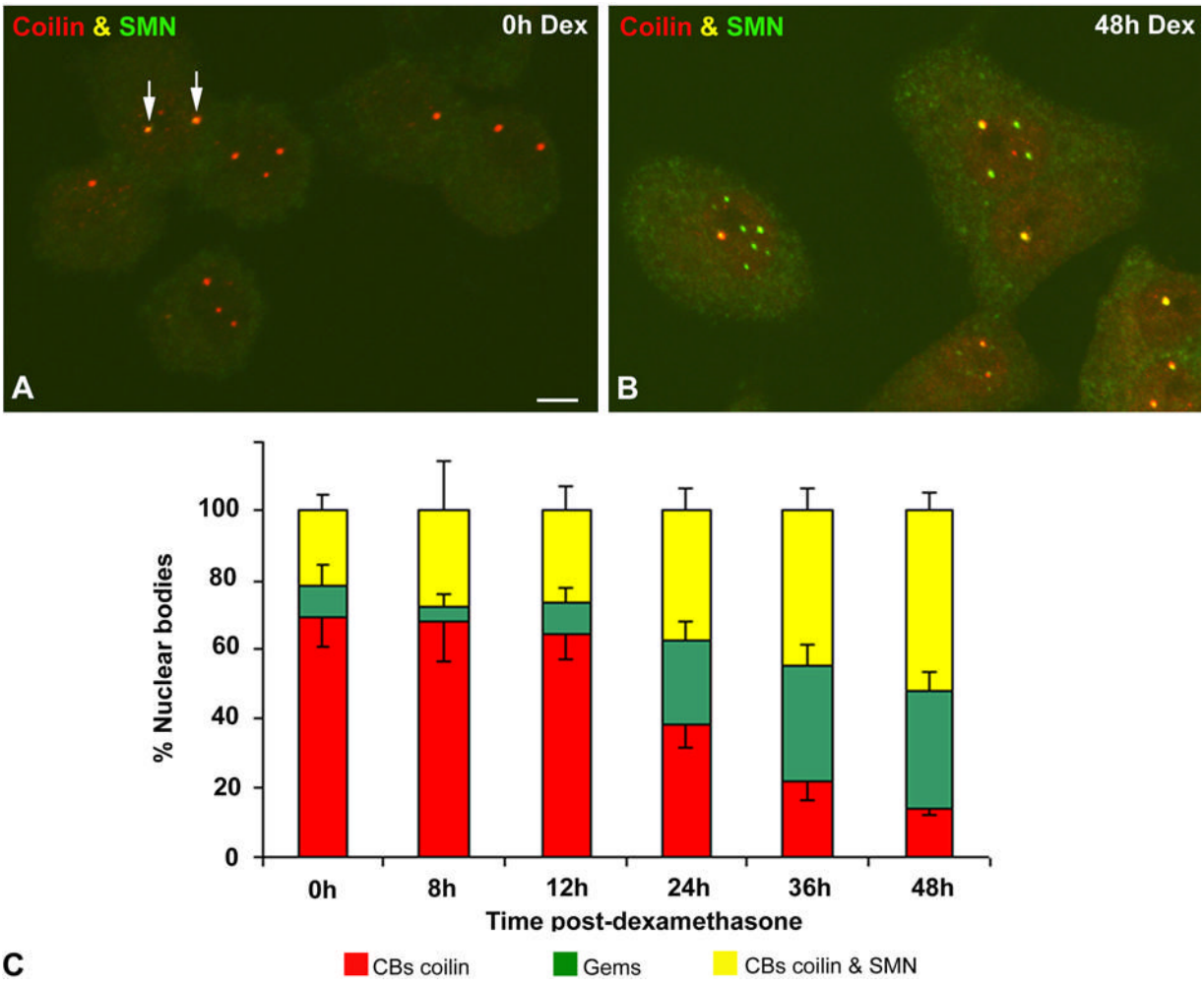

Fig. 2a-c.

Differentiation of UR61 cells induces a reorganization of Cajal bodies (CBs) and accumulation of gems. Representative examples of untreated (**a**) and dexamethasone-treated (**b**) UR61 cells costained for coilin and SMN (survival of motor neurons protein product). Most nuclear foci in untreated cells contain coilin-positive and SMN-negative CBs, whereas colocalization of both signals is only observed in a few CBs (arrows). By contrast, coilin and SMN colocalize in the majority of CBs upon dexamethasone-induced differentiation. This molecular reorganization of CBs is accompanied by the accumulation of SMN-positive foci (gems). Bar represents 3 μm. c Quantitative analysis of the distribution of the three categories of nuclear bodies, coilin-positive and SMN-negative (*red*), coilin-positive and SMN-positive (*yellow*) and gems (*green*), confirms the progressive accumulation of SMN in CBs and nuclear gems as differentiation proceeds (data are mean ± SD)

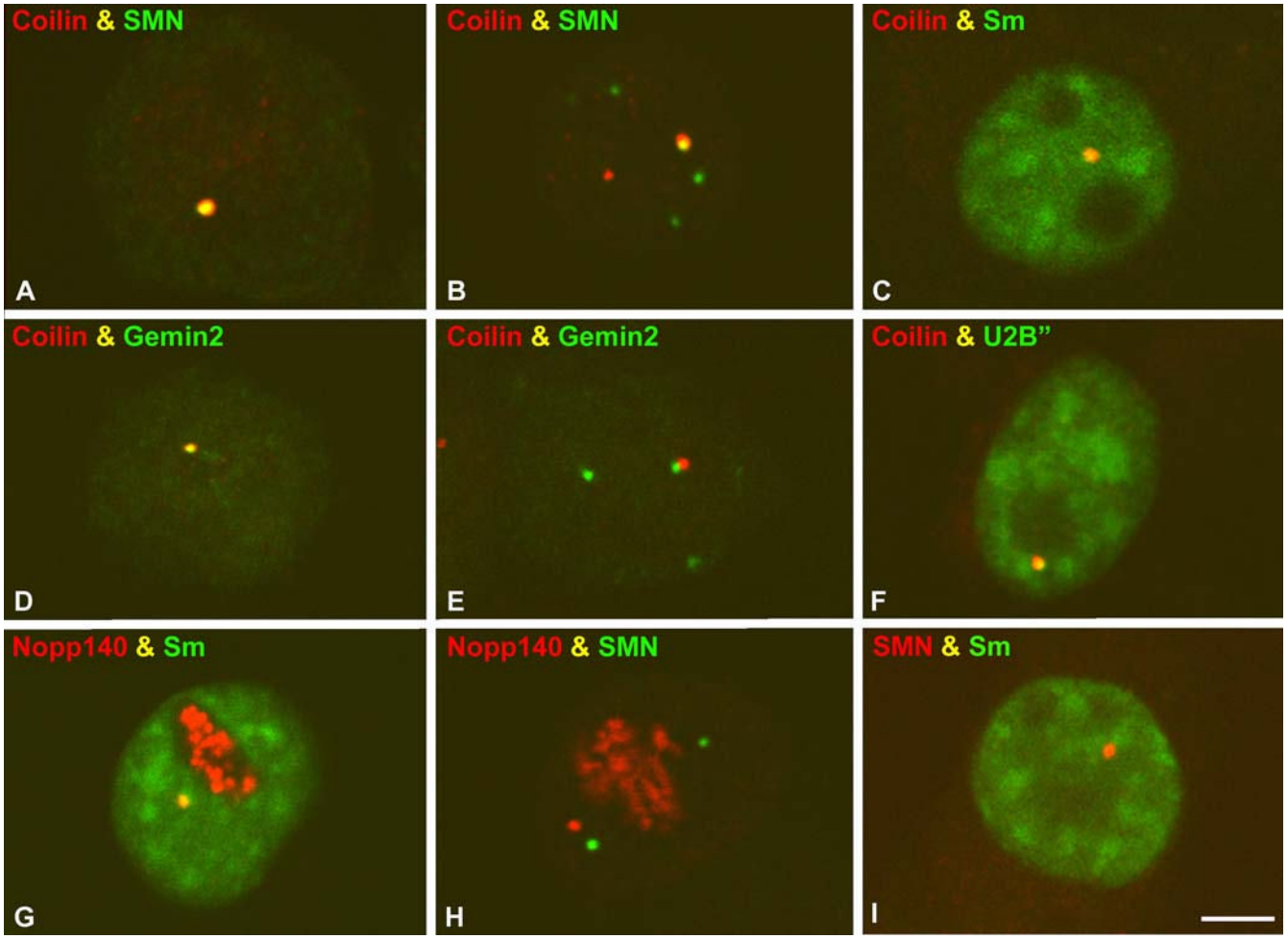

Fig. 3a-i.

Coilin-positive nuclear bodies in differentiated UR61 cells are bona fide Cajal bodies (CBs). All cell samples correspond to differentiated UR61 cells treated with dexamethasone for 36 h. Costaining experiments for different molecular constituents of CBs show that coilin foci colocalize with SMN (survival of motor neurons protein product) (**a,b**), Sm (**c**), Gemin 2 (**d**), and U2B" (**f**). The Sm complex also colocalizes with Nopp 140 (**g**) in the CBs of differentiated UR61 cells. Nuclear gems appear free (independent) in the nucleoplasm (**b, i**) or attached to coilin-positive nuclear foci (**e**), and are stained with antibodies against two components of the SMN complex, SMN protein (**b, h**) and Gemin 2 (**e**). The gems are also devoid of detectable Sm proteins (**i**). Bar represents 5 μm

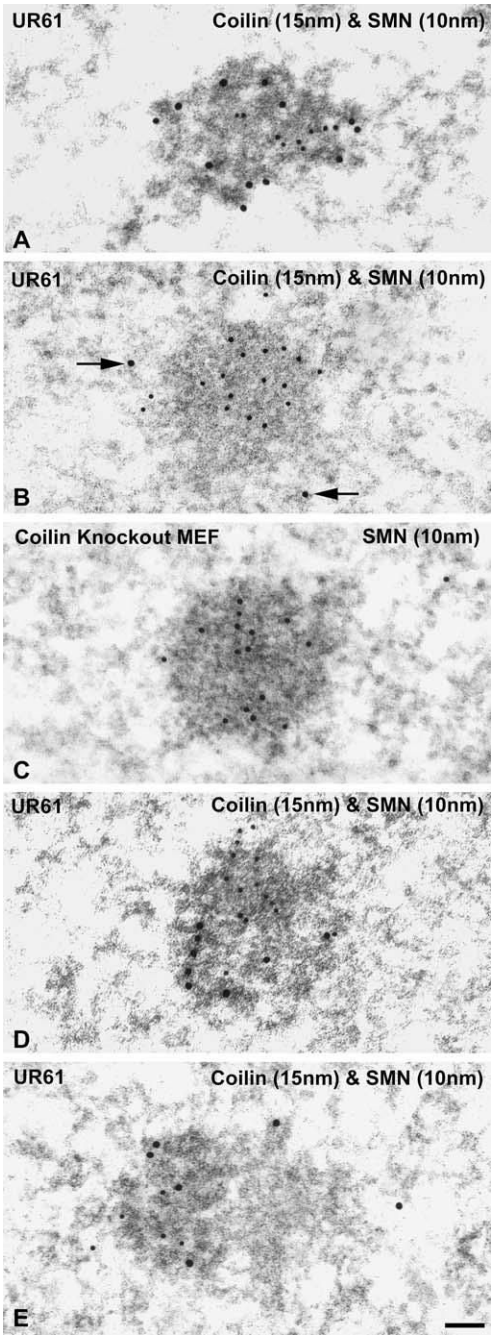

Fig. 4a-e.

Gems represent a distinct category of nuclear bodies by ultrastructural analysis. **a,b** Double immunoelectron labeling illustrating the distribution of coilin (large gold particles) and SMN (survival of motor neurons protein product; small gold particles) in nuclear bodies from differentiated UR61 cells upon 36 h of dexamethasone treatment. **a** A typical Cajal body (CB) composed of coiled dense threads appears decorated with large and small gold particles. **b** This nuclear body of granular nature and moderate electron density, identified as a gem, is only labeled with small gold particles, whereas some nucleoplasmic large particles (*arrows*) are seen in the vicinity of this body. **c** To confirm the ultrastructure of gems, we used the cellular model of MEF42, which does not contain coilin, but accumulates gems. Simple immunogold

labeling for SMN reveals an immunolabeled nuclear body (gem) identical to that described in **b** corresponding to a UR61 cell. **d** Double immunolabeling of a CB-gem pair in a differentiated UR61 cell. Large particles decorate the dense threads of the CB, whereas small particles appear segregated on the associated granular body. **e** This CB, double immunolabeled for coilin and SMN, has an associated mass of amorphous low density material free of both molecular constituents. Bar represents 100 nm

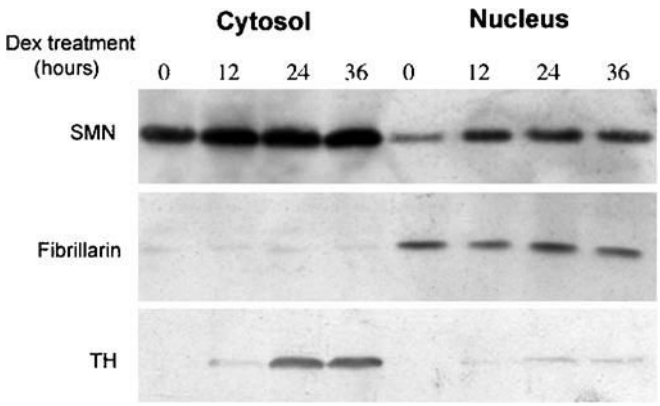

Fig. 5.

Differentiation of UR61 cells upregulates nuclear and cytoplasmic SMN (survival of motor neurons protein product). Immunoblot analysis of proteins extracted from nuclear and cytoplasmic fractions of UR61 cells using a mouse monoclonal anti-SMN antibody. Purity of subcellular fractions was checked using antibodies against tyrosine hydroxylase (TH, cytoplasm) and fibrillarin (nucleus). Dexamethasone (Dex)-induced differentiation increases the expression level of SMN in both nuclear and cytoplasmic fractions. Dexamethasone also induces a dramatic increase in the expression of tyrosine hydroxylase in cytoplasmic extracts

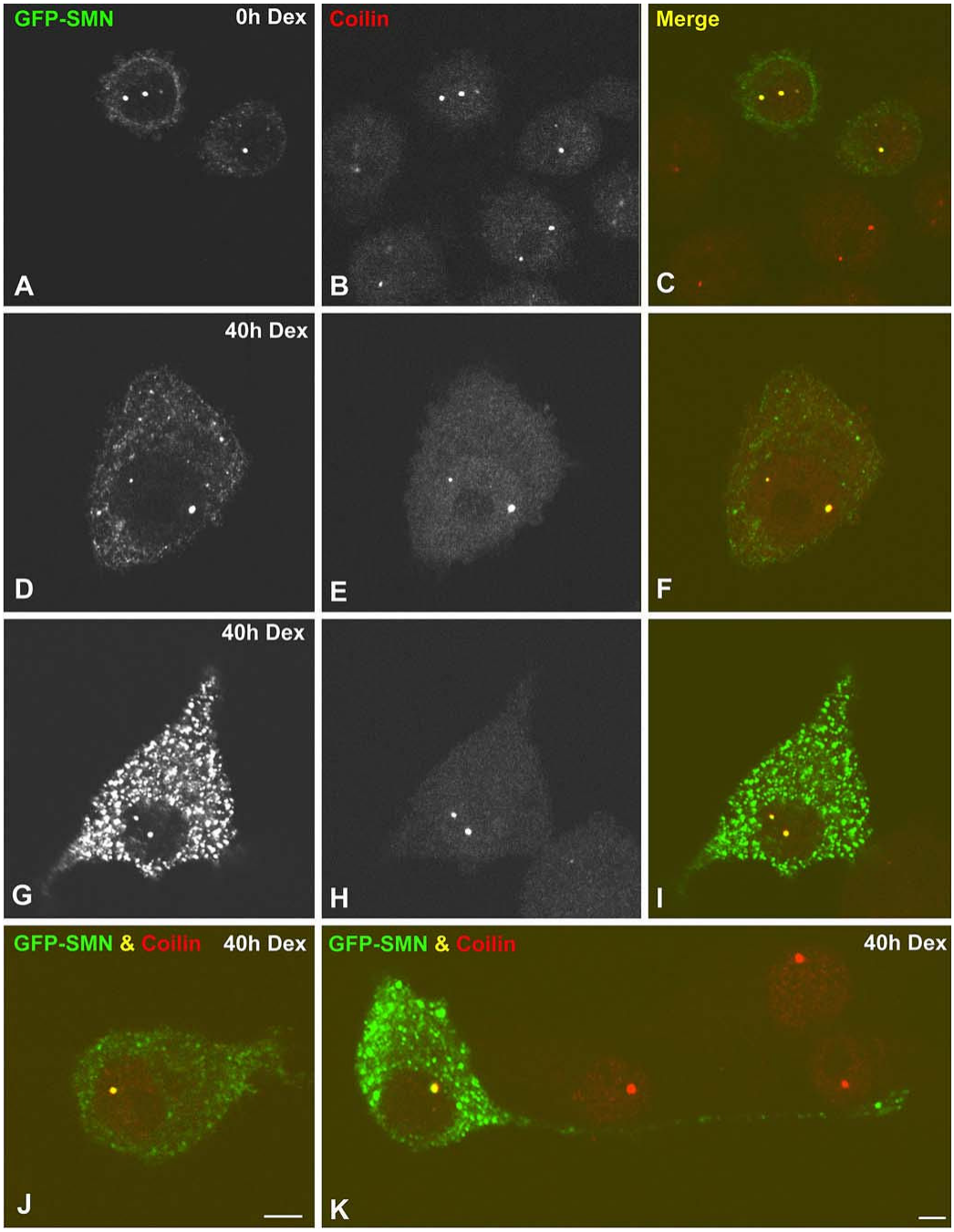

Fig. 6a-k.

Overexpression of GFP-SMN (green fluorescent protein-" survival of motor neurons protein product) in UR61 cells does not induce gem formation. Both undifferentiated (**a-c**) and differentiated (**d-k**) UR61 cells were transiently transfected with GFP-SMN and stained for coilin. GFP-SMN and coilin colocalize in all Cajal bodies (CBs) of transfected cells, whereas gems are not visible. Differentiated UR61 cells with low (**d-f**), moderate (**j**) and high (**g-i**) expression levels of cytoplasmic SMN show the same staining pattern of their nuclear bodies. **k** Numerous GFP-SMN aggregates appear distributed throughout the cytoplasm and within a long neurite in a differentiated UR61 cell. Bar represents 5 μm

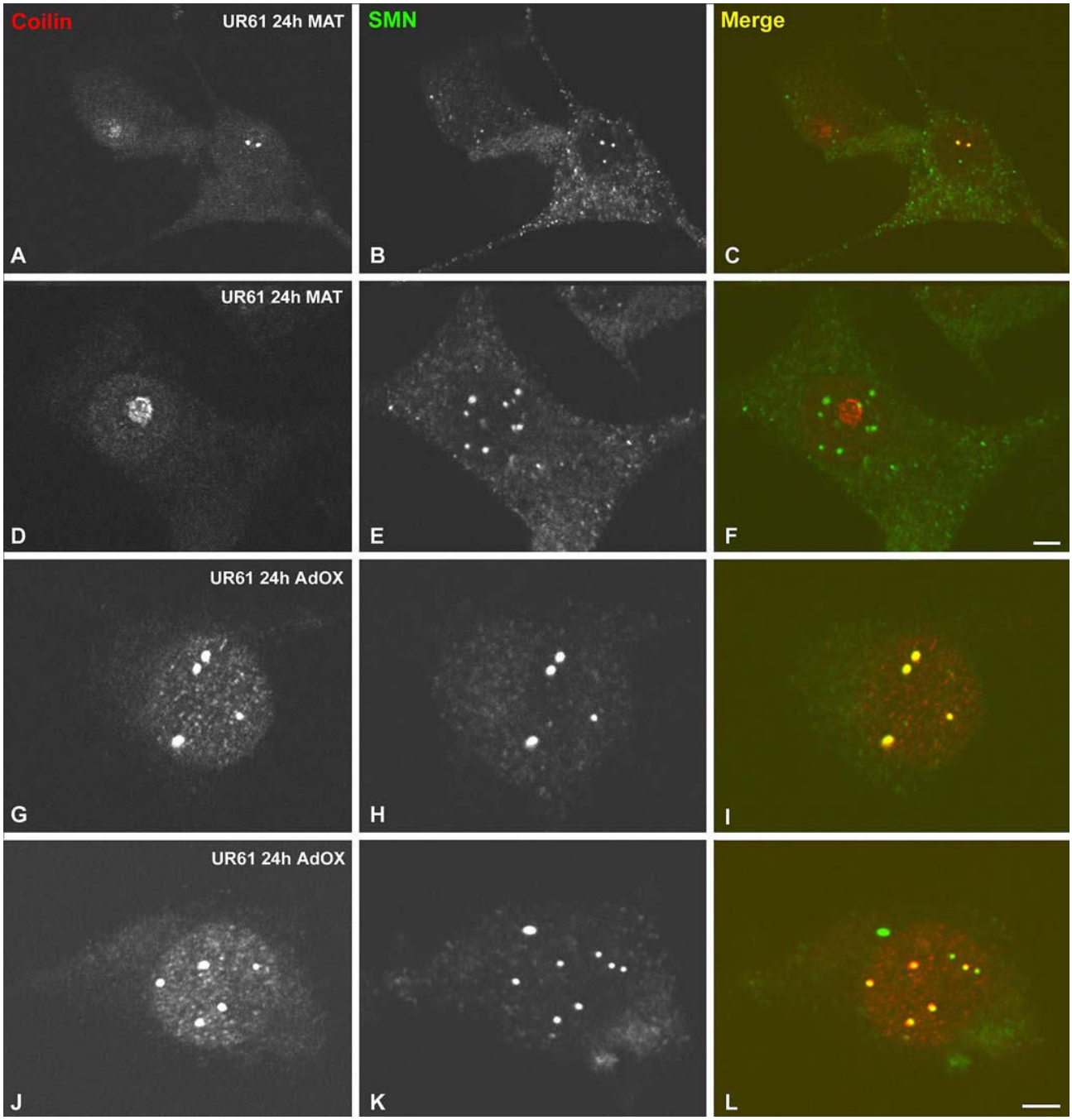

Fig. 7a-l.

Methyltransferase inhibitors induce formation of nuclear gems. Differentiated UR61 cells (upon 40 h of dexamethasone treatment) were incubated with either 5'-deoxy-5'-methylthioadenosine (MTA) (750 μM) or adenosine dialdehyde (AdOx) (100 μM) for 24 h. **a-f** Cells treated with MTA were costained for coilin and SMN. This treatment induces cytoplasmic accumulation of SMN (**a, c, d, f**), relocalization of coilin to the nucleolar periphery (**e, f**) and proliferation of gems (**d, f**). However, AdOx treatment induces the formation of numerous Cajal bodies (CBs), which appear costained for both coilin and SMN (**g-l**). Bar represents 5 μm

Table 1

Distribution of nuclear bodies in UR61 cells following treatment with methyltransferase inhibitors. (n=at least 200 in all groups; values are mean ± SDM) (AdOx,adenosine dialdehyde; Dex, dexamethasone; MTA, 5′-deoxy-5′-methylthioadenosine)

Cell type and treatment	Cajal bodies	Gems
UR61(0 h Dex)	1.65±0.25	0.13±0.12
UR61 (0 h Dex)+4 h MTA	1.56±0.10	0.09±0.06
UR61 (0 h Dex)+24 h MTA	1.20±0.11[a]	0.30±0.15
UR61 (0 h Dex)+4 h AdOx	1.50±0.08	0.06±0.05
UR61 (0 h Dex)+24 h AdOx	1.42±0.16	0.12±0.07
UR61 (40 h Dex)	2.00±0.23	1.10±0.39
UR61 (40 h Dex)+4 h MTA	1.79±0.22	0.87±0.22
UR61 (40 h Dex)+24 h MTA	1.10±0.05[b]	3.05±0.84[b]
UR61 (40 h Dex)+4 h AdOx	3.08±0.24[b]	0.68±0.23
UR61 (40 h Dex)+24 h AdOx	2.86±0.14[b]	1.19±0.44

[a]Significant differences ($p<0.005$) are found between untreated and MTA-treated groups of undifferentiated (0 h Dex) UR61 cells

[b]Significant differences ($p<0.005$) are found between untreated and MTA-treated or AdOx-treated groups of differentiated (40 h Dex) UR61 cells